On high pressure crystallization and the characterization of linear low-density polyethylenes

J. A. Parker, D. C. Bassett* and R. H. Olley
J. J. Thomson Physical Laboratory, University of Reading, Whiteknights, Reading, RG6 2AF, UK

and P. Jaaskelainen
Neste Oy Chemicals, PO Box 320, SF-06101 Porvoo, Finland
(Received 21 December 1993)

High pressure crystallization has been used to compare three linear low-density polyethylenes because of its potential for forming lamellae whose thicknesses are equal to the inter-branch separation. Major differences are revealed between one polymer prepared using a metallocene catalyst and the other two which have been generated by conventional Ziegler–Natta synthesis. The broad distribution of inter-branch lengths in the latter two polymers and the narrow spectrum of the former are revealed both by temperature rising elution fractionation (TREF) thermograms and the melting endotherms of the respective polymers after high pressure crystallization. The metallocene-catalysed polymer shows unprecedented behaviour in that its lamellar thickness is invariant. In consequence, it crystallizes at high pressure entirely as orthorhombic lamellae; the hexagonal phase is not formed.

(Keywords: linear low-density polyethylene; high pressure crystallization; short-chain branching)

INTRODUCTION

The importance of controlled degrees of short-chain branching in producing desirable properties in polyethylene is attested not only by the increasing quantities of linear low-density polymers manufactured but also by research which has led to greater control of branch location by using new catalysts. For the study of molecular structure/property relationships, however, linear low-density polyethylenes (LLDPEs) bring additional complications when compared to the linear material because of the need to characterize their branching distribution. One method for this which is widely used is temperature rising elution fractionation (TREF) which dissolves the more highly branched species at lower elution temperatures[1–3]. A second is crystallization at high pressure (typically 5 kbar, or 0.5 GPa). In this paper we compare three LLDPEs, one prepared by using a metallocene or single-site catalyst, with the others prepared by a Ziegler–Natta process, and show that the two methods of characterization are closely equivalent. We also confirm the regularity of the site distribution in the metallocene-catalysed polymer in a novel way and reinforce understanding of the fundamentals of high pressure crystallization of polyethylene.

MATERIALS AND TECHNIQUES

A metallocene-catalysed polyethylene, with 1-hexene as the comonomer, i.e. with butyl branches (polymer A), has been compared with two materials (polymers B and C) prepared by standard Ziegler–Natta catalysis using the same comonomer; all three materials were pilot-plant resins which were obtained from Neste Oy Chemicals. Their characteristics, which are listed in *Table 1*, show that polymers A and B have the same average branching ratio but different densities, while polymers A and C have the same density but different branching ratios.

Molecular characteristics

The molecular weights and their distributions were measured with a Millipore Waters 150 ALC/GPC machine. Two mixed bed and one 10^7 Å TSK-Gel columns were used. The instrument was operated at 135°C, with 1,2,4-trichlorobenzene (TCB) used as the eluent, and was calibrated with narrow-distribution polystyrene standards and broad distribution polyethylenes.

The comonomer and branching contents were determined by using either *FT*i.r. or n.m.r. spectroscopy. ^{13}C n.m.r. spectra were obtained on a Jeol GSX400 spectrometer, operating at 100 MHz at 135°C. A concentration of 300 mg of polymer in 5 ml of a 9:1 mixture of TCB and hexadeuterobenzene (lock solvent) was used, with tetramethylsilane being employed as the chemical shift reference. The *FT*i.r. measurements were made on pressed films, using a Nicolet 510 Fourier transform i.r. spectrometer. The intensity of the methyl absorbance at 1378 cm^{-1} was measured using the second derivative of this peak; the instrument was calibrated by the use of ^{13}C n.m.r. spectroscopy.

* To whom correspondence should be addressed

0032-3861/94/19/4140–06

Table 1 Characteristics of the three linear low-density polyethylenes investigated in this study

	Polymer		
	A	B	C
Density (kg m^{-3})	922	929.6	920.7
Comonomer[a] content (wt%)			
n.m.r.	5.4	5.6	–
*FT*i.r.	–	5.4	8.6
Branch content[b]	9.6	9.7	15.1
HDPE type of material (%)[c]	0	28	28
M_n	42 700	27 300	30 000
M_w	96 500	121 000	140 000
M_w/M_n	2.3	4.4	4.7
T_m (°C)	116.2	126.7	126.1
Crystallinity (%)[d]	46.9	51.7	45.7
T_{cr} (°C)	102.1	112.8	110.8

[a] 1-Hexene
[b] Expressed as number per 1000 C atoms
[c] Calculated from TREF curves
[d] Calculated by d.s.c.

The calorimetric measurements reported in *Table 1* were made with a Mettler TA4000/DSC30 instrument on 3 mg samples in a nitrogen atmosphere. These were melted at 180°C for 5 min, cooled at a rate of 10 K min^{-1} to 0°C, and then remelted by heating at a rate of 10 K min^{-1} over the temperature range 0–180°C. The crystallinities were estimated from the enthalpies of fusion by assuming a value of 290 J g^{-1} for perfectly crystalline material. Density measurements were carried out at 23°C using the ASTM D1505 density gradient method.

Characterization by TREF

Fractionation of the LLDPE resins was achieved by using analytical temperature rising elution fractionation (TREF). The TREF profiles were generated using an instrument built at Neste Oy Chemicals which was similar to a published design[3]. The sample was dissolved in xylene (2–4 mg ml^{-1}) at 130°C and injected into the column at 130°C, and the latter was then cooled to 20°C at a rate of 1.5 K h^{-1}. The column was subsequently eluted with TCB at a flow rate of 0.5 ml min^{-1} while the temperature was increased from 20 to 130°C over 4.5 h. The output, detected with an i.r. detector operating at a wavelength of 3.41 μm, was presented as a fractogram normalized to constant area.

High pressure crystallization

Crystallization from the melt at high pressure (4.9_5 kbar, 0.49_5 GPa) was carried out in a piston-cylinder apparatus with samples accommodated in a cylindrical volume (5 cm long and 1.5 cm in diameter) containing silicone oil as a pressure transmitting fluid[4]. The samples themselves were sheets (~0.5 mm thick) which had been moulded from the original pellets and mounted in the cylinder immersed in the silicone oil. Similar sheets of all three of the polymers A B and C were placed side by side, melted under high pressure, and then crystallized while cooling at a rate of ~1.5 K min^{-1} under the controlled high pressure. When the temperature had returned close to ambient, pressure was released, the samples were removed, washed in acetone and dried, and then examined morphologically and by thermal analysis.

Thermal analysis

Melting endotherms of samples before and after high pressure crystallization were recorded with a differential scanning calorimeter (Perkin–Elmer model DSC-2C) operating at a scanning rate of 10 K min^{-1}, with calibration against high purity indium.

Morphology

A limited amount of morphological information was gained by the examination of thin (5 μm) microtomed sections with a polarizing microscope. For the most part, however, samples were examined after permanganic etching[5,6], either with Nomarski differential interference contrast optics in reflection, by scanning electron microscopy (SEM) or, for best resolution, by using two-stage replication and transmission electron microscopy (TEM).

Two permanganic reagents were used: the one for general inspection contained 0.7% w/v of potassium permanganate dissolved in a mixture of 2 volumes of concentrated sulfuric acid and 1 volume of dry orthophosphoric acid, while the system for highest lamellar resolution contained 1% w/v of potassium permanganate in a mixture of 10 volumes of concentrated sulfuric acid, 4 volumes of orthophosphoric acid and 1 volume of water. In both cases, after etching for ~1 h, the samples were washed according to published procedures[5] and then dried ready for microscopic examination.

RESULTS

Examination of the three polymers by TREF showed a clear distinction between materials prepared by the two types of catalyst (*Figure 1*). Samples B and C show a wide response across some 60 K, ending with a narrow peak of half-width ~2.5 K; sample A shows a single peak, with a half-width of ~5 K and a slightly skew base, which is just under 30 K wide.

Thermal analysis of the three polymers in their original (sheet) form produced three similarly shaped curves (*Figure 2*) with peak melting points increasing, in the order A–C–B, while the half-widths decrease in the order A–B–C. However, recrystallization at 5 kbar causes major changes. The three polymers then show endotherms (*Figure 3*) which are qualitatively similar to their TREF curves in that A shows but a single peak, whereas B and C have similar extended endothermic responses. For the

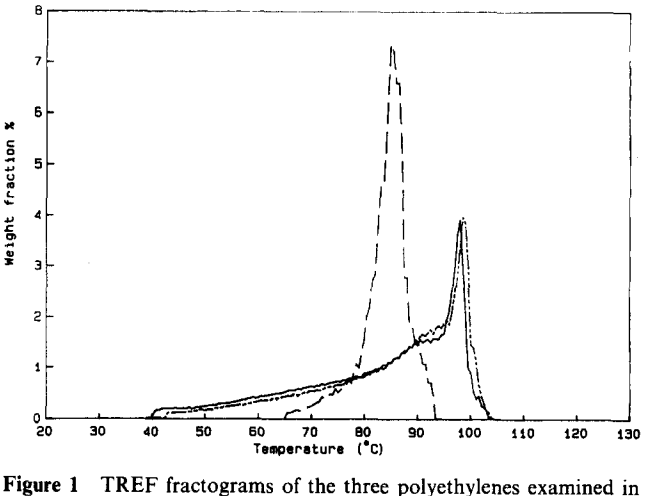

Figure 1 TREF fractograms of the three polyethylenes examined in this study: (– –) A; (– – – –) B; (——) C

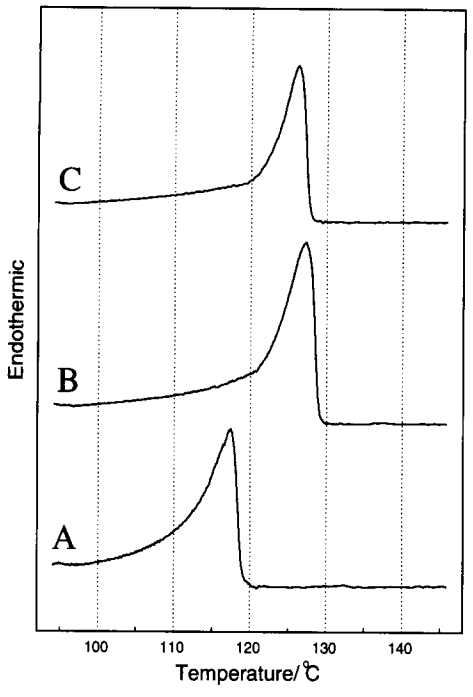

Figure 2 Melting endotherms of the original polyethylene materials

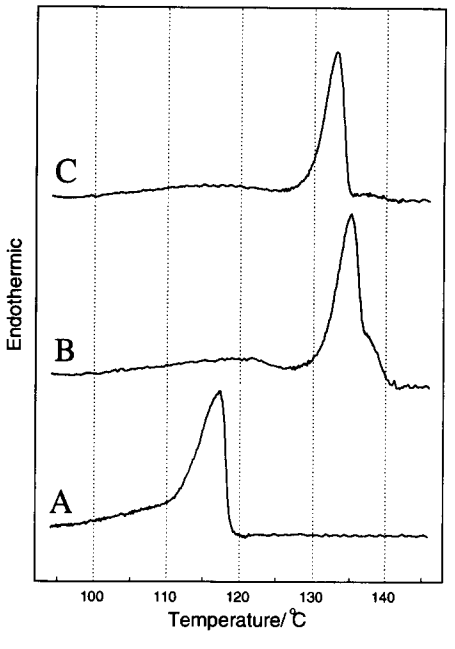

Figure 3 Melting endotherms obtained after recrystallization of the three polyethylenes at 5 kbar

latter two, there is a broad region over ~20 K to 125°C, a major central peak, then a high temperature region, seen as a shoulder for B but being much reduced for C. In accordance with previous experience[7–9] the central peaks of B and C are substantially raised in temperature when compared to the starting material. This is not the case for polymer A for which high pressure recrystallization has caused no upward shift of the peak melting temperature, merely a narrowing of the peak. In our experience, such behaviour is unprecedented.

The morphologies of the three polymers before and after high pressure treatment (*Figure 4*) support and amplify these differences. Beforehand, the lamellar shapes and organization, although not identical, all show features which are characteristic of crystallization of branched polyethylene from the melt directly as the orthorhombic form[4]. Afterwards, the polymers B and C show mixed morphologies in which there is an additional component characteristic of crystallization via the two-dimensional hexagonal or high pressure phase. This has a spiky, elongated appearance and is present within a matrix whose lamellar habit identifies it as having crystallized directly into the orthorhombic phase[4]. Completely different, and again unprecedented in our experience, is the appearance of polymer A after high pressure crystallization. This consists entirely of banded spherulites and shows that polymer A has crystallized from the melt at 5 kbar wholly into the orthorhombic form; there is no evidence of involvement of the hexagonal phase.

DISCUSSION

This work has concentrated on the use of high pressure crystallization to characterize branched polyethylenes. The underlying reason is that this treatment tends to produce very thick lamellar crystals in polyethylene. For linear and methyl-branched polymers, the thickness is typically of the order of micrometres, but can be very much more. On the other hand, lamellar thickness is much reduced for branched polyethylenes containing ethyl or larger branches[10]. In previous, unpublished work, two of us have shown that such branches are excluded from crystals first formed as the hexagonal phase so that the inter-branch separation gives an upper limit to the lamellar thickness[7–9]. The crystallization procedure adopted here, namely slow cooling from the melt at 5 kbar, is designed to allow approach to the limiting situation in which branched molecules are fully extended within a lamella, with adjacent branches located on opposite fold surfaces.

This preamble leads to the expectation that the melting endotherm after high pressure recrystallization will be a representation of the inter-branch lengths and thus the branching distribution in the polymer, albeit subject to the details of the crystallization process. In that case, there should be at least a qualitative similarity to the TREF curves. These are based on solubility, but of a polymer also crystallized sequentially on cooling; moreover, for a crystalline polymer dissolution is equivalent to melting plus dispersal. With rising temperature, the more-branched molecules are eluted which, for Ziegler–Natta catalysis, tend also to be those of a lower molecular weight[11].

Melting endotherms are also measures of lamellar thickness distributions so that increases in the melting point upon high pressure recrystallization mirror the corresponding changes in lamellar thickness. For the random copolymers B and C, there have been considerable increases in lamellar thickness due, in part, to crystallization via the hexagonal phase, although, as discussed below, the majority of each sample still crystallizes as the orthorhombic phase, but at a reduced supercooling when compared to the original. The invariance of the melting point of polymer A, despite the extreme recrystallization conditions, is thus in agreement with the claims that branching in metallocene-catalysed polyethylenes is regularly disposed along the molecular chain and that butyl branches are excluded from the orthorhombic lattice.

The separation between the branches of polymer A may be estimated from the branch content and compared

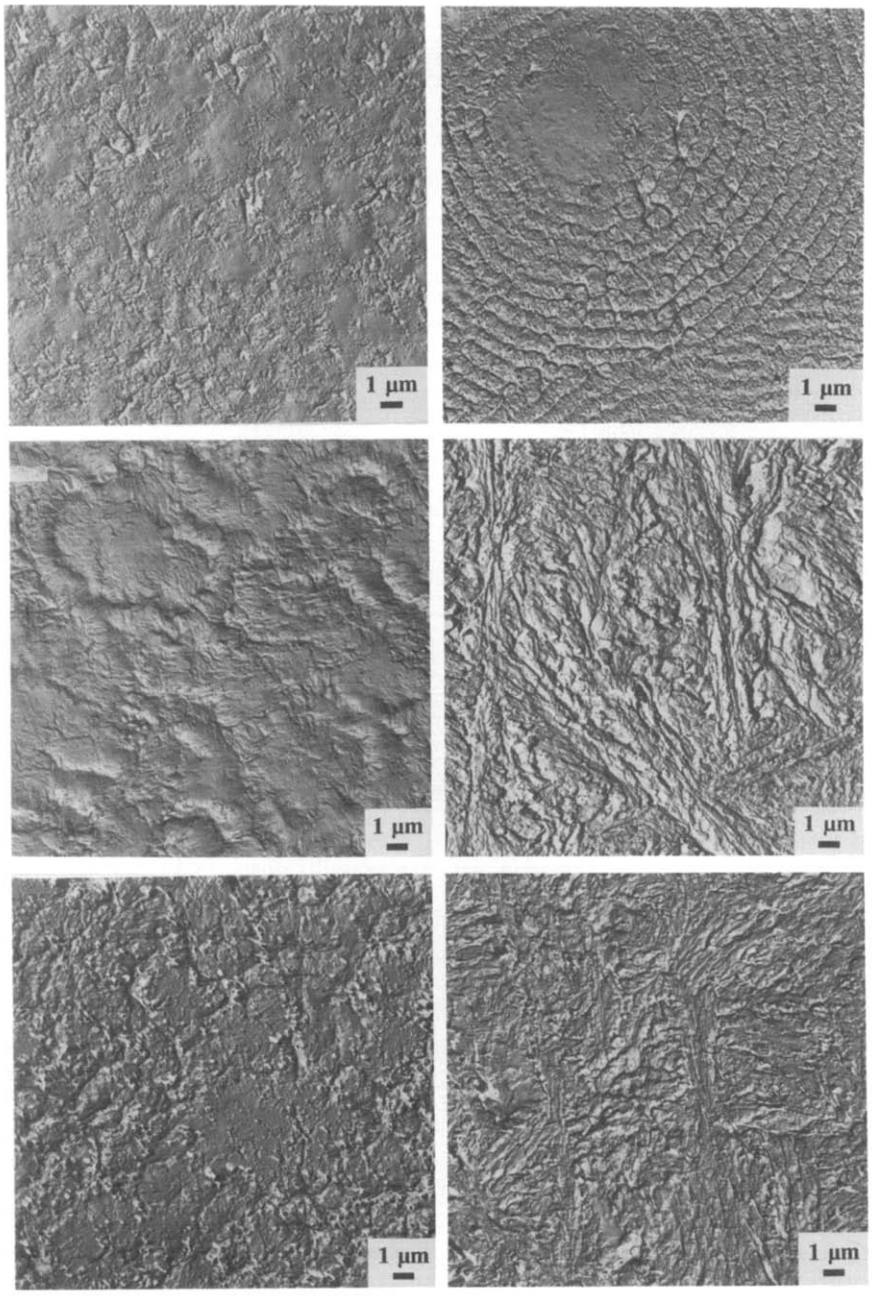

Figure 4 Electron micrographs showing the morphologies, after permanganic etching, of the three polyethylenes before (left-hand side) and after (right-hand side) recrystallization at 5 kbar. Top, polymer A; centre, polymer B; bottom, polymer C

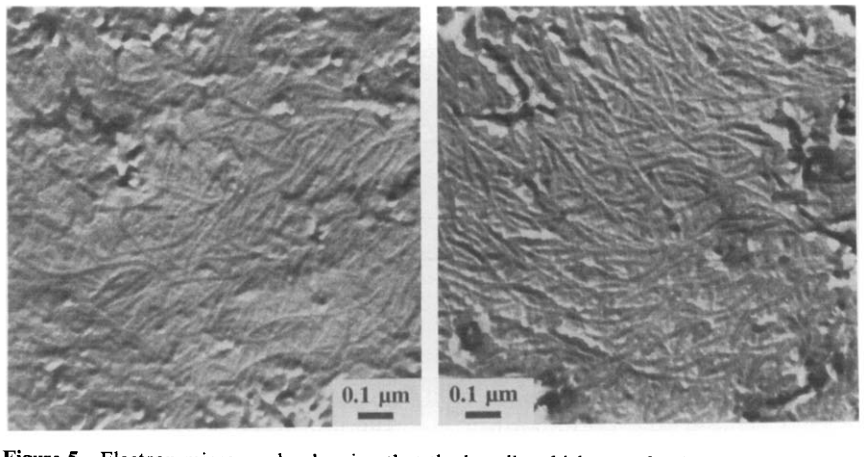

Figure 5 Electron micrographs showing that the lamellar thickness of polymer A is the same before (left-hand side) and after (right-hand side) recrystallization at 5 kbar

with values derived from the melting point data and from electron microscopy. A branch content of 9.6 per 1000 carbon atoms (*Table 1*), with each being 1.27 Å apart, along the *c*-axis of the unit cell leads to a lamellar thickness (l) as follows:

$$l = \frac{1000}{9.6} 1.27 \cos\theta = 132 \cos\theta \text{ (in Å)}$$

where θ is the angle between the *c*-axis and the lamellar normal. For $\theta = 35°$, a value typically found in polyethylene[12], the value of l would be 108 Å. Substitution in the melting point equation:

$$T_m = T_m^0(1 - 2\sigma_e/\Delta h l)$$

using the parameters $T_m^0 = 415$ K, $\sigma_e = 93$ mJ m^{-2} and $\Delta h = 300$ J cm^{-3}, yields, for a melting temperature of 117°C, a value for l of 103 Å. Lamellar thicknesses resolved by electron microscopy (*Figure 5*) are also in agreement with these values. The situation is thus self-consistent, although there is scope for future consideration of how the precise nature of the lamellae and their molecular constitution might be better defined by a more exacting comparison of more comprehensive data.

High pressure crystallization

We consider now the distinction between the behaviour of polymers A, B and C in the context of the understanding of high-pressure-crystallization phenomena in polyethylene. Of particular interest is the inference that while polymers B and C crystallized from the melt at 5 kbar partly as the disordered hexagonal phase and partly as the orthorhombic, polymer A crystallized only in the orthorhombic form.

The inference is based on the morphological distinction which led to the prediction, then discovery, of the high pressure phase of polyethylene. It was shown first that high pressure crystallization of a given linear polyethylene gave a product with two discrete, non-overlapping, melting ranges and that while the lower-melting-range material had spherulitic textures which were familiar from growth at atmospheric pressure, the upper-melting-range material had a characteristically spiky texture[4]. Moreover, the two textures correlated not only with different exothermic patterns and supercoolings for crystallization[13], but also with different X-ray reflections[14], all recorded *in situ* at pressure. It was thus predicted (and confirmed) that the coarse spiky morphology is formed by the hexagonal phase crystallizing from the melt in contrast to the finer spherulitic texture created by crystallization directly into the orthorhombic phase.

The crystallization of polymers B and C at 5 kbar produces a composite texture with limited amounts of hexagonally crystallized polymer (see *Figure 4*). The proportion appears less for C than for B, as would be expected from their respective branching ratios. This is in agreement with the sizes of the highest melting peak in *Figure 3*, i.e. the one lying in the range 135–140°C. The remainder of the polymers B and C, plus all of polymer A, crystallized directly into the orthorhombic phase. It is useful to discuss here why this should be. There are three principal factors involved: the relative chemical potentials (specific Gibbs functions) of the three phases, the concept of kinetically competing crystallization processes, and the influence of the basal surfaces of lamellae responsible *inter alia* for lowering the melting

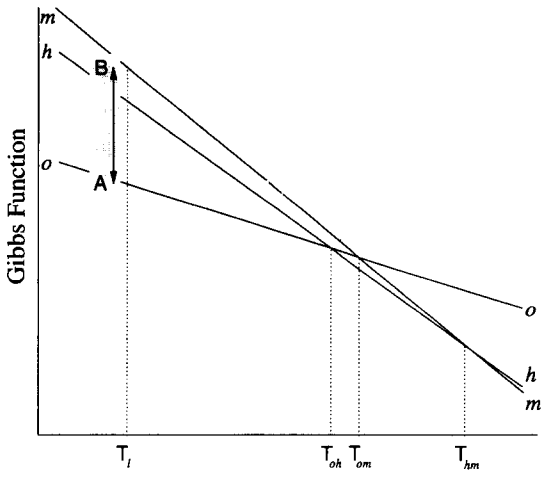

Figure 6 A schematic representation of the variation with temperature of the Gibbs function of polyethylene, measured at 5 kbar

point of thin crystals, and known in that context as the Gibbs–Thomson equation.

The chemical potentials of the bulk melt, hexagonal and orthorhombic phases are shown schematically in *Figure 6*, in which the curvature of the lines is neglected, i.e. the entropies are assumed not to vary with temperature, or alternatively, that the specific heat capacities are zero. Previous work on linear polyethylenes[13] found that crystallization at 5 kbar began, for ultra-high-molecular-weight polymer, at only 2.5 K below T_{hm}, with the corresponding exothermic d.t.a. peak 5 K below this temperature. These supercoolings increased for lower pressures to ~12 K at 3 kbar where, at a cooling rate of ~1 K min^{-1}, direct formation of the orthorhombic phase began to occur. This process gave exothermic peaks at a supercooling of 15–20 K (with respect to T_{om} below the triple point), depending on the pressure and the grade of polymer.

The supercoolings at which polymer A crystallized at 5 kbar must have been substantially in excess of these figures. This follows because crystallization of a lamella has to occur below its melting point. At 1 bar and a cooling rate of 0.62_5 K min^{-1}, parallel experiments have shown that the exothermic d.s.c. peak is 10 K below the melting point of 117°C, i.e. at 35 K of supercooling; at 5 kbar, lamellae of A have the same thickness and will, therefore, show at least the same depression of melting point as at 1 bar. (It will be the same if the entropy of fusion is invariant with pressure, but more if this entropy decreases with pressure and more still, by ~25%, if the enthalpy of fusion does not change.) One may thus expect a depression (with respect to the melting point of infinitely thick orthorhombic lamellae, T_{om}) of at least 25 K, i.e. the atmospheric figure. Crystallization will occur at still greater supercoolings, of at least 35 K, i.e. ~210°C, if the atmospheric crystallization rates are taken as a guide. These are supercoolings which are roughly twice those for the change from hexagonal to orthorhombic crystallization at ~1.5 K min^{-1} cited above, and some three times that observed for slower isothermal growth. In other words, the thinness of the A lamellae, which is dictated by the exclusion of butyl branches, depresses the thermodynamically allowed crystallization temperature to a value well into the region where only orthorhombic lamellae grow.

This situation is depicted in *Figure 6*, in which AB represents the Gibbs function associated with the depression of the melting point, for crystals of thickness l, to T_l. The crystallization temperature, T_c, is thus restricted to $T_c < T_l$. Normally in experiments involving crystallization of linear polyethylene at 5 kbar it is difficult, because of the large thermal masses which impose slow rates of cooling, to reach temperatures low enough for crystallization of the high pressure (hexagonal) phase to have given way to direct crystallization of the orthorhombic phase. However, this has been achieved when the particular apparatus being used allowed sufficiently high cooling rates[15], thus giving the same result as reported here, namely crystallization as banded spherulites, previously shown to be characteristic of orthorhombic growth. With the metallocene-catalysed polymer A, we have, therefore, reached the same region of the phase diagram for crystallization, but by having now a specific molecular architecture which will not allow crystallization until these low temperatures are reached.

The situation regarding the Ziegler–Natta catalysed polymers B and C may be similarly understood, but in this case in terms of random short-chain branching. Polymer B, which has the same average figure for the branching ratio as A, must therefore include components with higher and lower ratios than A. Polymer C would be expected to be similar, but with the branching spectrum shifted to higher values (i.e. lower elution temperatures in a TREF thermogram, as shown in *Figure 1*). The more highly branched molecules would thus have to crystallize at still lower temperatures than are allowed for A, because l would be lowered to below 100 Å. This would move the relevant T_l further to the left in *Figure 6*. Conversely, T_l for the less branched molecules would move to the right in this figure. For sufficiently long inter-branch lengths, T_l would reach a value high enough for crystallization of the hexagonal phase to occur.

Our data present a consistent picture in this respect. Not only is there the morphological indication of spiky hexagonally derived textures, with a lesser amount for C than for B, but also the orthorhombic morphologies of B and C indicate crystallization over a range of supercoolings. In addition, there is the evidence of a wide spread of melting points in *Figure 3*. A peak figure of 135°C, i.e. a 7 K depression, would be expected to bring the associated crystallization temperature into the supercooling region of 15 K or less, in which hexagonal crystallization has been observed to occur[13]. For as long as crystallization is limited by crystal thickness (inter-branch separation), it is immaterial for the atmospheric melting point as to which phase the polymer first crystallized, so that the melting endotherm would be continuous. Only if inter-branch lengths are significantly longer than the thickness of the secondary nucleus at the crystallization temperature will the possibility exist of subsequent lamellar thickening. Especially in the hexagonal phase, this would increase the eventual atmospheric melting point. The upper shoulders on the melting endotherm for B and C in *Figure 3* may well arise in this way and represent the only departure from crystallization limited by inter-branch separations.

These findings are also relevant to a recent discussion of high pressure crystallization of polyethylene[16] in which the regions of stability implicit in the Gibbs–Thomson equation have been made explicit in the context of the polyethylene phase diagram. Nevertheless, in practice it is kinetics rather than thermodynamics which determine the phase which develops, i.e. the one which grows faster. We have, accordingly, presented our new findings in relation to the extensive kinetic data, for pressures from 5 kbar to below the triple point, reported in previous work[4,13].

CONCLUSIONS

The principal conclusions of this paper, which has compared three linear low-density polyethylenes, are as follows:

1. High pressure crystallization is a complementary technique to TREF for revealing branch distribution.
2. Metallocene-catalysed polymer has a much more regular distribution of branches than that produced by the Ziegler–Natta synthesis.
3. Butyl branches are excluded from the hexagonal and orthorhombic lattices and make the crystal thickness of A invariant at the inter-branch separation of 10 nm.
4. Crystallization of lamellae, constrained to be 10 nm thick, from the melt at 5 kbar is restricted to low temperatures, at which the orthorhombic phase forms directly from the melt.

REFERENCES

1 Wild, L. *Adv. Polym. Sci.* 1991, **98**, 1
2 Bonner, J. G., Frye, C. J. and Capaccio, G. *Polymer* 1993, **34**, 3532
3 Wild, L. *Trends Polym. Sci.* 1993, **1**, 50
4 Bassett, D. C. and Turner, B. *Philos. Mag.* 1974, **29**, 285
5 Olley, R. H., Hodge, A. M. and Bassett, D. C. *J. Polym. Sci. Polym. Phys. Edn.* 1979, **17**, 627
6 Olley, R. H. and Bassett, D. C. *Polymer* 1982, **23**, 1797
7 Olley, R. H. and Bassett, D. C., unpublished results
8 Bassett, D. C. 'Principles of Polymer Morphology', Cambridge University Press, Cambridge, 1981, p. 133
9 Bassett, D. C. in 'Developments in Crystalline Polymers 1' (Ed. D. C. Bassett), Applied Science, London, 1982, p. 115
10 Bassett, D. C. in 'Developments in Crystalline Polymers 2' (Ed. D. C. Bassett), Applied Science, London, 1988, p. 67
11 Jaaskelainen, P. and Lehtinen, A. International Symposium on Polymer Analysis and Characterisation, Brno, Czechoslovakia, July, 1990, p. 135
12 Bassett, D. C. and Hodge, A. M. *Proc. R. Soc. London A* 1981, **25**, 377
13 Bassett, D. C. and Turner, B. *Philos. Mag.* 1974, **29**, 925
14 Bassett, D. C., Block, S. and Piermarini, G. J. *J. Appl. Phys.* 1974, **45**, 41
15 Rees, D. V. and Bassett, D. C. *J. Polym. Sci. (A-2)* 1971, **9**, 385
16 Rastogi, S., Hikosaka, M., Kawabata, H. and Keller, A. *Macromolecules* 1991, **24**, 6384